SUPPLEMENTARY INFORMATION (SI) APPENDIX

The conserved autoimmune-disease risk gene *TMEM39A* regulates lysosome dynamics

Shuo Luo[1], Xin Wang[1], Meirong Bai[1], Wei Jiang[1], Zhe Zhang[1], Yifan Chen[2], Dengke K. Ma[1,3,*]

[1]Cardiovascular Research Institute, University of California San Francisco, San Francisco, CA 94158

[2]Department of Molecular and Cell Biology, University of California Berkeley, Berkeley, CA 94720

[3]Department of Physiology, University of California San Francisco, San Francisco, CA 94158

*Correspondence and requests for materials should be addressed to D.K.M.

dengke.ma@ucsf.edu

This PDF file includes:

Detailed Methods (page 2 to 8)

Supplemental Figures 1 to 3 (page 9 to 14)

Movie Legends (page 15)

Table S1 (page 16)

Supplemental References (page 17)

Detailed Materials and Methods

C. elegans culture and strains. All *C. elegans* strains were handled and maintained at 22°C as described previously unless otherwise specified (1). The N2 Bristol strain was used as the wild-type, and genotypes of strains used are listed as below:

LGI: *tmem-39(dma258, dma268, dma308(WS->AA))*

LGII: *nIs617[tts-1$_p$::gfp, unc-54$_p$::mCherry]*

LGV: *zcIs4[hsp-4$_p$::gfp]*

LGX: *vsIs48[unc-17$_p$::gfp], oxIs12[unc-47$_p$::gfp]*

Unknown linkage: *dmaIs45[rpl-28p::mCherry::pdr-1], dmaIs47[rab-3$_p$::lmp-1::Venus, unc-54$_p$::mCherry], dmaIs57[hsp-16.48$_p$::mCherry::tmem-39, unc-54$_p$::mCherry], dmaIs58[rpl-28$_p$::lmp-1::Venus, unc-54$_p$::mCherry], sqIs19[hlh-30$_p$::hlh-30::gfp], pwIs503[vha-6$_p$::mans::GFP + Cbr-unc-119(+)], wdIs52[F49H12.4::GFP + unc-119(+)]*

Extrachromosomal arrays: *dmaEx594[tmem-39$_p$::mCherry::tmem-39; unc-122$_p$::GFP]*

Generating tmem-39 knockin and knockout C. elegans *strains through CRISPR-Cas9.* The following oligos were used to generate the *tmem-39(dma258)* deletion allele:

sgRNA-EcoRI-F: ttgtaaaacgacggccagtgaattcCTCCAAGAACTCGTACAAAAATG;

sgRNA-HindIII-R: ctatgaccatgattacgccaagcttCACAGCCGACTATGTTTG;

TMEM-39 sgRNA1 F: GCCGCCTCGAAGACGAGTGCGTTTAAGAGCTATGCTGGAAACAGC;

TMEM-39 sgRNA1 R: GCACTCGTCTTCGAGGCGGCAAACATTTAGATTTGCAATTCAATTA;

TMEM-39 sgRNA2 F: GATCTACGAACCTTCTCAAGGTTTAAGAGCTATGCTGGAAACAGC;

TMEM-39 sgRNA2 R: CTTGAGAAGGTTCGTAGATCAAACATTTAGATTTGCAATTCAATTA;

TMEM-39 deletion donor oligo:

aagatATGCCGCCTCGAAGACGAG^AAGAGGATCTTCTCCTTATGCATCAACTTCAACAAGAAC GATAA;

The following oligos were used for genotyping: fw- tacagaaccgagaaggtcac; rv- tcacaattgggtagtaccac; nest primer- GTGTGAACTGAATATCCGGC. The Addgene plasmid #46169 was used as template to amplify sgRNA fragments. The *tmem-39* target sequences in the oligos are underlined. The sgRNAs generate a precise deletion of 2750 bp.

To generate the *tmem-39(dma268)* early stop codon allele, the 100bp chemically modified sgRNA cctcctattgcgagatgtcttGGCTTCAATCCCAAGAGCGAGgtttaagagctatgctgg was ordered directly from Synthego and the single-strand donor DNA oligo ACGAGTGCCGGCACCTCCACCACAAGCTCCTTCCGTGCCAGCT**TAA**ATCCCA**TGA**GCGAGTC GTGTAACGCTTTCCGTCCATCCTATATGGCCGGATATT was ordered from IDTDNA as 4 nM ultramer, with the *tmem-39* target sequence underlined and stop codons being bold. The oligos fw-ccagtctacagagccggatt and rv- AGAAACAGACGGTTACCCTC were used for genotyping. The insertion of stop codons was confirmed by sequencing.

To generate the *tmem-39(WS->AA)* knockin allele, the following oligos were used to amplify the *tmem-39* targeting sgRNA:

WS->AA sgRNA F: TAGAGACAAAACTCGCTCCAGTTTAAGAGCTATGCTGGAAACAGC;

WS->AA sgRNA R: TGGAGCGAGTTTTGTCTCTAAAACATTTAGATTTGCAATTCAATTA;

and the PvuII(CAGCTG)-containing repair donor template AATTGGCCATACTGGAAGTATGAGCTCGGCTCCAACGCCAGCTGCCGAGTTTTGTCTCTATA ATGACGGAGAGACTGTTCAAATGCCGGACGGCAGGTGC was used to introduce the WS-to-AA knockin. The oligos fw-GCCCGTAAGTGCCTTCAGTA and rv-TGGTCAAGGTGAAGCAGTTG were used for amplifying a 994 bp *tmem-39* fragment and the mutation was confirmed by PvuII digestion and sequencing.

To generate knockout and knockin alleles, one day old wild type adult animals were injected with injection mixture containing 5 μM sgRNA, 5 μM Cas9 nuclease (IDT), 50 ng/μl ssODN repair template, 2.5 ng/μl pCFJ90 (*myo-2$_p$::RFP* as co-injection marker) and 300 mM KCl, which were homogenously mixed and incubated at room temperature for 10 minutes before injection. RFP-expressing F1 animals were transferred to fresh OP50-spotted NGM plates and allowed to give rise to progeny, and F2 animals that were dumpy and had strong *hsp-4$_p$::gfp* expression were recovered. All alleles were confirmed by genotyping and sequencing.

Germline transformation. Transgenic lines were constructed using standard germline transformation procedures (2). All DNA samples were injected at a final concentration of 10 ng/μL with 5 ng/μL of *unc-54$_p$::mCherry* or *unc-122$_p$::4×NLS::gfp* as a co-injection marker and 100 ng/μL of pcDNA3. For transgene integration, transgenic strains carrying extrachromosomal arrays were irradiated with UV and integrated lines were confirmed by the expression of co-injection marker in 100% of their progeny.

RNAi treatments. RNAi experiments were performed as described previously (3, 4). Briefly, HT115 *E. coli* strains carrying individual RNAi clones were cultured overnight in LB liquid media supplemented with 75 mg/L ampicillin. 100 μL of bacterial culture were seeded onto 6 cm NGM plates supplemented with 1 mM IPTG and 75 mg/L ampicillin, which were then incubated at room temperature (22°C) for overnight (>12 hrs) to allow expression of siRNA. For RNAi experiments, three to five L3-L4 larvae were transferred to RNAi plates and allowed to give progeny at 22°C for three to four days. The F1 progeny were then examined for desired phenotype. Bacteria expressing the empty RNAi vector pL4440 were used as a control.

Cell culture. The HEK293T cells were maintained in DMEM (MT-10-013-CV, Thermo Fisher Scientific) supplemented with 10% FBS (10-437-028, Thermo Fisher Scientific) and grow at 37°C with 5% CO_2. For transient transfection, cells were seeded in 24-well plates with cover glass (22293232, Fisher Scientific), and 400 ng of each target plasmids were transfected into the cells with presence of polyethylenimine (PEI 25000, 23966-1 PolyScience). The cells were fixed 24 hours after transfection with 4% formaldehyde solution for 15 mins at room temperature, washed with 1×PBS, and sealed on microscope slide with Fluoroshield Mounting Medium with DAPI (NC0200574, Thermo Fisher Scientific) for imaging.

Generating TMEM39A knockout HEK 293T cells through CRISPR-Cas9. The following oligos were used to generate the *TMEM39A* knockout HEK 293T cells:

TMEM39a_sgRNA_prom_fw, caccgACAAAGCCCCTATGCCTTTG;

TMEM39a_sgRNA_prom_rv, aaacCAAAGGCATAGGGGCTTTGTc;

TMEM39a_sgRNA_exon2_fw, caccgGGCTTAGCTGTTGCCGACTA;

TMEM39a_sgRNA_exon2_rv, aaacTAGTCGGCAACAGCTAAGCCc;

The first sgRNA targets around 600 bp upstream of the human *TMEM39A* 5'-UTR, and the second sgRNA targets the 2nd exon of *TMEM39A*. The sgRNAs were annealed and cloned into plasmid-based sgRNA-expressing vectors as previously described (5). The sgRNAs and Cas9 protein (IDT) were incubated at RT to form ribonucleoprotein (RNP) complex before being transfected into wild-type HEK 293T cells. The transfected HEK 293T cells were clonally screened for *TMEM39A* deletion using the following oligos:

TMEM39a_prom_geno_fw, atccagtgcctgacacaaca;

TMEM39a_prom_geno_rv, tggaagagaggcgacactaag;

TMEM39a_exon2_geno_fw, ggcctgcttactcagtgtttg;

TMEM39a_exon2_geno_rv, gggcaggatttctaccacag.

Successful *TMEM39A* knockout clones containing various lengths of deletions were confirmed by PCR and sequencing.

DYNC1I2 knockdown by lentiviral-mediated shRNA expression. Lentiviral shRNA plasmids targeting human DYNC1I2 were obtained from Sigma-Aldrich (Sigma-Aldrich, SHCLNG-NM_001378):

5'- CCGGCCCTGTTATACAGATAATGTTCTCGAGAACATTATCTGTATAACAGGGTTTTTG - 3'(TRCN0000116797, 3'UTR),

5'- CCGGGCAGGTGCTAAACTGTCATTACTCGAGTAATGACAGTTTAGCACCTGCTTTTTG - 3'(TRCN0000116799, CDS),

5'- CCGGGCAGACTATGTTTATGATGTTCTCGAGAACATCATAAACATAGTCTGCTTTTTG - 3'(TRCN0000116800, CDS),

5'- CCGGTCTTCAGCTTCACTCAGATTCCTCGAGGAATCTGAGTGAAGCTGAAGATTTTTG- 3'(TRCN0000296596, CDS),

5'- CCGGTTTGGGACGAGGACCTATTAACTCGAGTTAATAGGTCCTCGTCCCAAATTTTTG - 3'(TRCN0000296603, CDS).

To package lentivirus, HEK293T cells were transiently transfected with pMD2.G, psPAX2 and shRNA plasmids at ratio of 1:2:3. The lentivirus-based GFP-specific shRNA was used as negative controls (Addgene 31849). Forty-eight hours after transfection, viral particles-containing media was collected, filtrated through 0.45 μm syringe filter (Millipore EMD, SLHP033RS) and incubated with fresh 293T cells at 37 °C for 6 hours in the presence of 10 μg/mL Polybrene (Sigma-Aldrich TR-1003-G). Stably infected cells were enriched by 1.5 μg/mL puromycin for 3 days. The knockdown efficiency of DYNC1I2 was evaluated by imaging and Western blot.

Microscopy and colocalization analysis. Nomarski DIC and epifluorescence images were obtained using EVOS inverted microscope (Fig. S1B, S3D; Life Technologies) or Leica CTR5000 compound microscope (Fig. 1D, 3A, 4C, 4E, S1D, S2C, S2I, S3A; Leica). Confocal images were obtained using Zeiss LSM 700 (Fig. 2H, 2I, S2H) or Leica SPE microscope (all other confocal images). Images were processed and quantified using Fiji software (NIH). The colocalization analysis (Fig. 2B-C, S2A-B, S2E-G) was performed using the JACoP plugin within Fiji as described previously (6). Briefly, grayscale images in gfp and mCherry channels were opened in JACoP and the background fluorescence was adjusted using Costes' automatic threshold. Pearson's Correlation Coefficient was calculated based on the selected region of interest (ROI). The whole image was used for colocalization analysis when ROI was not specified. The fluorescence intensity plots (Fig. 2C, S2B) were generated using the Leica LAS X imaging software (Leica).

Immunoprecipitation. HEK293T cells were seeded in 3.5 cm culture dishes and transiently transfected with plasmids expressing GFP::TMEM39A and DYNC1I2::V5. Twenty-four hours after transfection, cells were washed with 1× ice-cold PBS and lysed with 400 μL 1×CLB lysis buffer (Cell Signaling) in the presence of 10 mM PMSF and protease inhibitor cocktail (BioTools, B14002) at 4˚C for 60 minutes. The lysate was then centrifuged at 13,000 rpm for 15 mins to remove cell debris. To precipitate GFP::TMEM39A proteins, lysate was incubated with 4 μL of pre-clean magnetic beads (Chromotek, bmab-20) at 4°C for 15 minutes, followed by incubation with 8 μL of GFP-trap magnetic beads (Chromotek, gtma-100) at 4°C for 1-2 hours. The beads were then washed with 400 μL of 1× CLB lysis buffer for 5 times and resuspended in 40 μL of 1× Laemmli Sample Buffer. The samples were then boiled at 95°C for 10 minutes and subject to Western blot analysis.

Western blots. For autophagy analysis, HEK293T cells were grown to 90%-100% confluence in 24-well tissue culture plates and treated based on experimental needs before being lysed directly in 100 µL 1× Laemmli Sample Buffer. Proteins were resolved by 4-15% gradient SDS-PAGE (Bio-Rad, 4561086) and transferred to nitrocellulose membrane using semi-dry transfer system (Bio-Rad, 1620167). Proteins of interest were then detected using antibodies against Beclin-1 (Cell Signaling Technology, 3738S), Ser15-P-Beclin-1 (Cell Signaling Technology, 84966), GFP (Abbkine, A02020), mCherry (ThermoFisher Scientific, M11217), V5 tag (EMD Millipore, AB3792) or β-tubulin (Sigma, T5168).

Yeast two-hybrid. To screen for TMEM39A interacting proteins, the cDNA coding sequence corresponding to the second cytoplasmic loop of human TMEM39A (a.a. 341-418) was cloned into the pGBKT7 vector and screened against a normalized universal human cDNA library (Clontech, 630481) following manufacturer's instructions (Clontech, Matchmaker® Gold Yeast Two-Hybrid System, 630489). Positive colonies growing on –Ade/-His/-Leu/-Trp quadruple synthetic dropout (SD) plates were verified by plasmid recovery and yeast re-transformation following manufacturer's protocol (Clontech). To image protein interactions, single yeast colonies that grew on double or quadruple dropout plates were resuspended in H_2O and respotted onto fresh –Ade/-His/-Leu/-Trp quadruple dropout plates. The plates were incubated at 30°C for 2 days before growth of yeast patches was captured using a smartphone camera (Huawei P10 Lite). The yeast images were processed using Windows10 Photos (Microsoft).

Statistical analysis. Data are presented as means ± S.E.M. The P values were calculated by unpaired Student's t-tests.

A

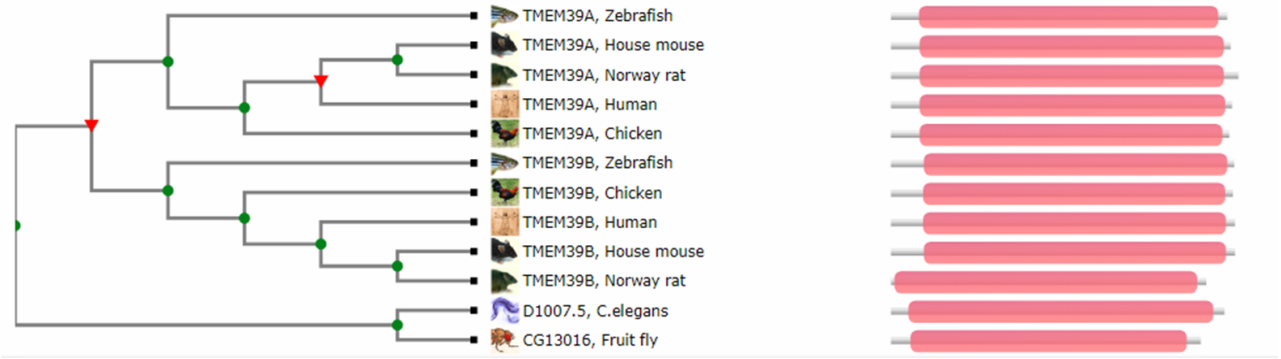

B

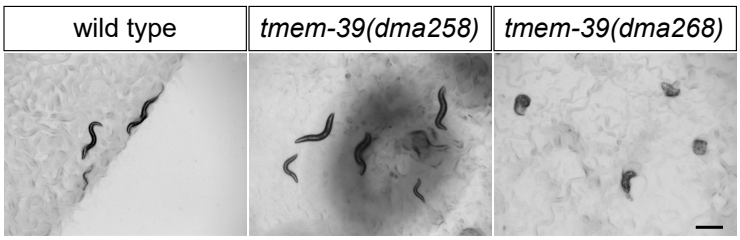

C

Genotype	% of animals bursting*	*n*
Wild type	0	100
tmem-39(dma258)	2	100
tmem-39(dma268)	56	100

*: Assayed at 25°C.

D

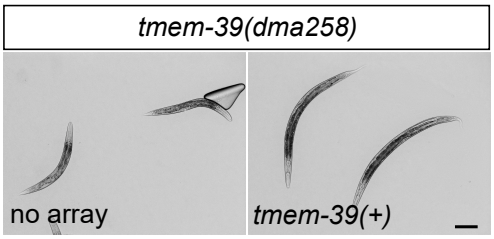

E

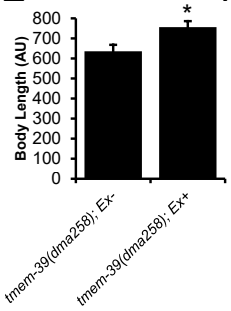

F

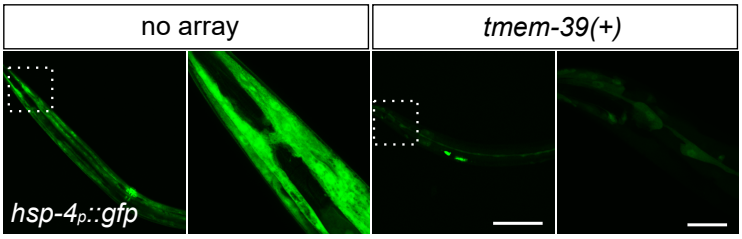

G

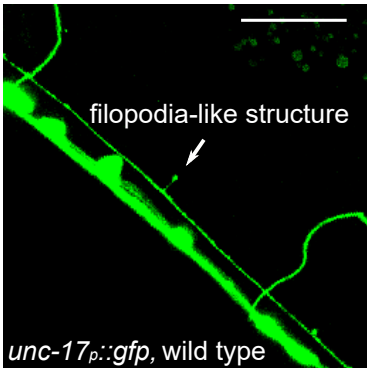

H

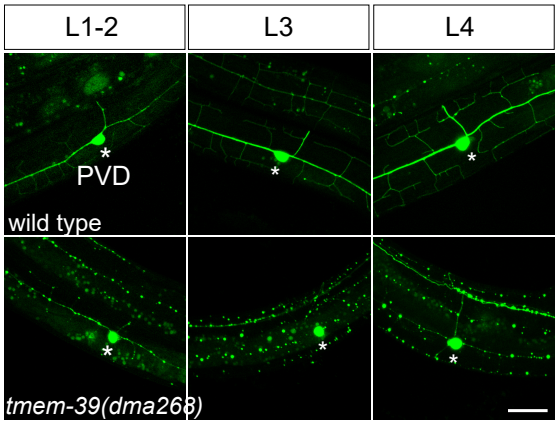

Supplemental Figure 1. *tmem-39* mutant animals show developmental defects that are rescued by *tmem-39* transgene. *A*) Cladogram showing conservation of the TMEM39A protein sequences throughout evolution. The cladogram is retrieved from Treefam (http://www.treefam.org/family/TF321110#tabview=tab1), and the red boxes represent conserved multi-transmembrane domains. *B*) Animals deficient in *tmem-39* are dumpy and tend to burst when growing at 25°C, indicating defects in hypoderm development. Scale bar, 500 μm. *C*) Quantification of bursting phenotype of *tmem-39* mutant animals. *D*) Expression of *tmem-39* genomic sequence restores normal body length of *tmem-39* mutant animals. Scale bar, 100 μm. *E*) Quantification of rescue of body length in *D*). Data represent mean ± S.E.M.; *, $P<0.05$. *F*) Expression of *tmem-39* rescuing transgene suppresses *hsp-4$_p$::gfp* ER stress reporter activation. Scale bar, 100 μm, enlarged images 20 μm. *G*) Representative confocal image showing the filopodia-like structure in wild-type adults that express the cholinergic *unc-17$_p$::gfp* reporter. Scale bar, 20 μm. *H*) Confocal images showing the PVD neuron in wild-type and *tmem-39* mutant animals at different developmental stages. The PVD neuron is generated in *tmem-39* mutants (asterisk), whereas PVD dendrites show signs of degeneration-like morphological abnormality in early larval animals. Scale bar, 20 μm.

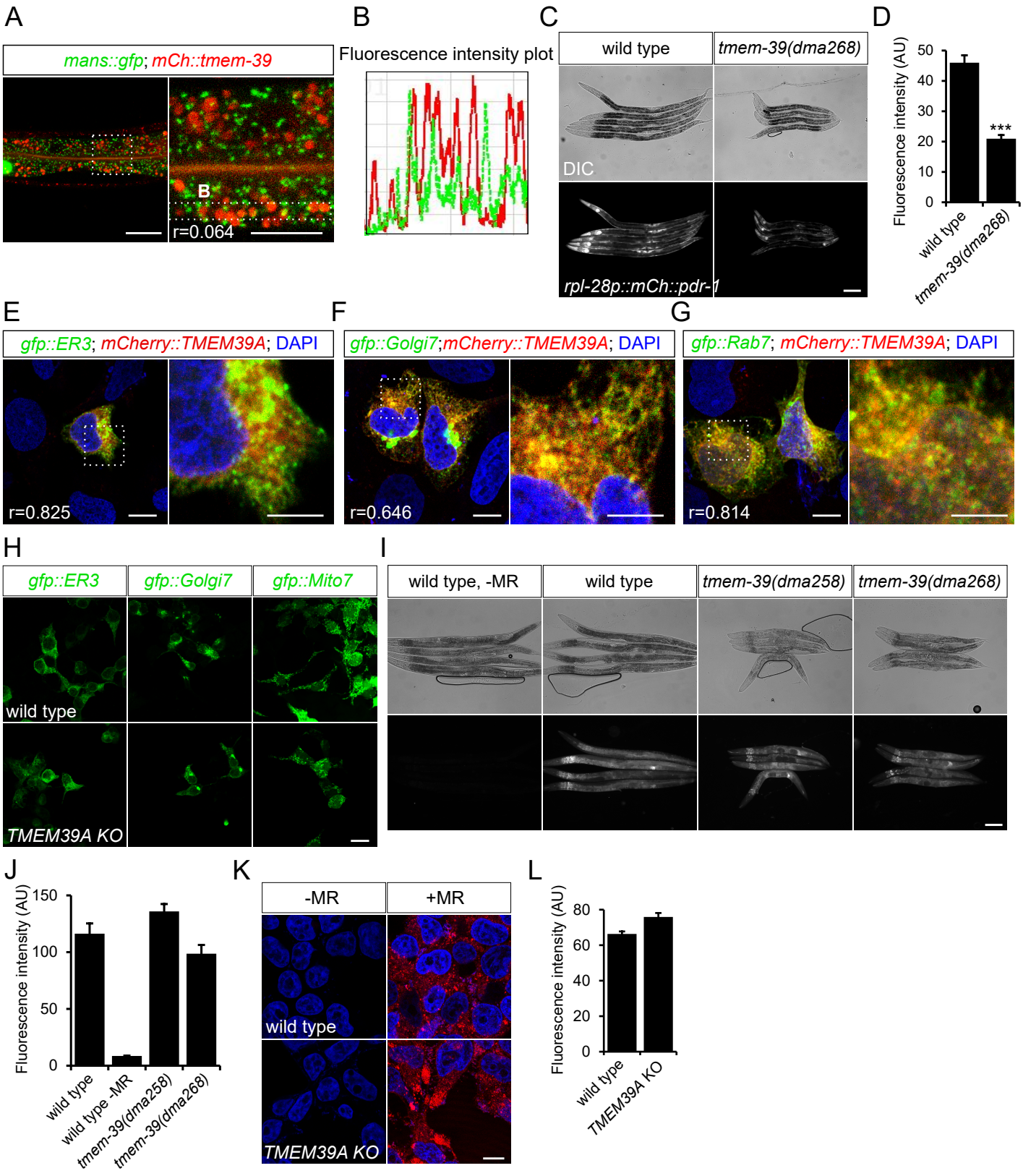
A
mans::gfp; mCh::tmem-39
B
r=0.064
B
Fluorescence intensity plot
C
wild type
tmem-39(dma268)
DIC
rpl-28p::mCh::pdr-1
D
Fluorescence intensity (AU)
50
40
30
20
10
0
***
wild type
tmem-39(dma268)
E
gfp::ER3; mCherry::TMEM39A; DAPI
r=0.825
F
gfp::Golgi7;mCherry::TMEM39A; DAPI
r=0.646
G
gfp::Rab7; mCherry::TMEM39A; DAPI
r=0.814
H
gfp::ER3
gfp::Golgi7
gfp::Mito7
wild type
TMEM39A KO
I
wild type, -MR
wild type
tmem-39(dma258)
tmem-39(dma268)
J
Fluorescence intensity (AU)
150
100
50
0
wild type
wild type -MR
tmem-39(dma258)
tmem-39(dma268)
K
-MR
+MR
wild type
TMEM39A KO
L
Fluorescence intensity (AU)
80
60
40
20
0
wild type
TMEM39A KO

Supplemental Figure 2. TMEM39A partially co-localizes with lysosomes in human cells and deficiency in TMEM39A does not affect lysosome enzymatic activity. *A*) Confocal images showing non-overlapping expression pattern of mCherry::TMEM-39 and Golgi-localized MANS::GFP. The Pearson's Correlation Coefficient (r=0.064) indicates that TMEM-39 is not significantly associated with Golgi apparatus at least in the *C. elegans* intestine. Scale bar, 20 μm; enlarged image, 10 μm. *B*) Intensity plot of mCherry::TMEM-39 and MANS::GFP fluorescence in the boxed region in a). *C*) Compound fluorescence images showing decreased expression of mCherry::PDR-1 under the *rpl-28* promoter in *tmem-39* mutant animals, indicating that disruption of *tmem-39* does not induce P*rpl-28*-mediated transcription upregulation. Scale bar, 100 μm. *D*) Quantification of mCherry::PDR-1 fluorescence in wild type and *tmem-39* mutant animals. Data represent mean ± S.E.M.; ***, $P<0.001$. *E-G*) Confocal images of transiently transfected HEK293 cells showing partial co-localization of mCherry::TMEM39A with ER and Golgi reporters as well as late endosome/lysosome marker Rab7. Quantification of the colocalization reveals a strong association of mCherry::TMEM39A protein with ER (r=0.825) and Rab7-labeled late endosomes/lysosomes (r=0.814) and to a lesser extent with Golgi apparatus (r=0.646). Scale bar, 10 μm; enlarged images, 5 μm. *H*) Confocal images showing comparable localization of ER, Golgi and mitochondrial markers in wild type and *TMEM39A* KO cells, suggesting disruption of TMEM39A does not cause gross morphological abnormalities of these subcellular compartments. Scale bar, 20 μm. *I*) Magic red staining of wild type and *tmem-39* mutant animals reveals comparable lysosome enzymatic activity as represented by cathepsin B-mediated substrate cleavage. Scale bar, 100 μm. *J*) Quantification of the Magic red staining in *I*). Data represent mean ± S.E.M. *K*) Magic red staining of wild type and *TMEM39A* KO HEK293T cells reveals no apparent difference in lysosome activity as represented by cathepsin B-mediated substrate cleavage. Similar to gfp-tagged lysosome reporter, Magic red staining enriches at cell periphery of *TMEM39A* KO cells, consistent with lysosome re-distribution. Scale bar 10 μm. *L*) Quantification of the Magic red staining in *K*). Data represent mean ± S.E.M.

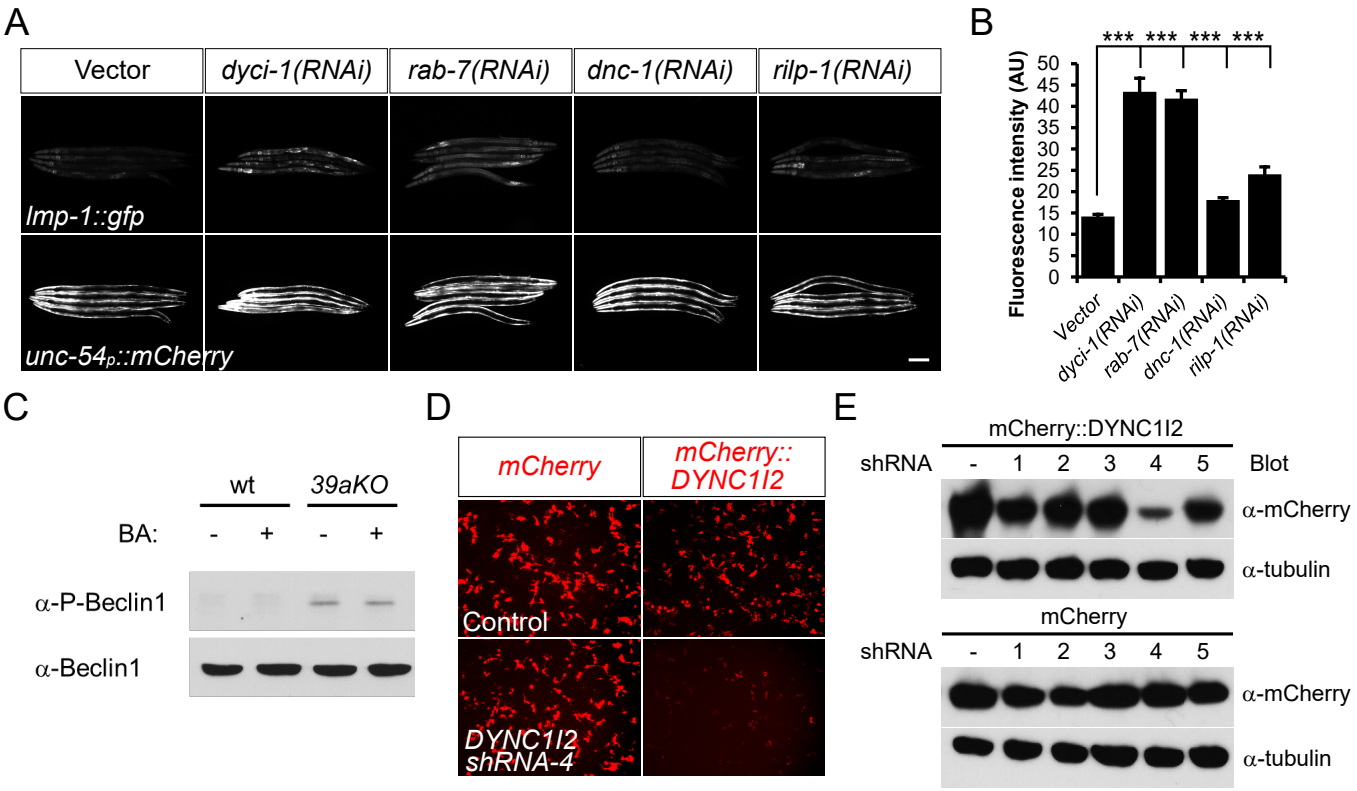
A
Vector
dyci-1(RNAi)
rab-7(RNAi)
dnc-1(RNAi)
rilp-1(RNAi)
lmp-1::gfp
unc-54p::mCherry
B
Fluorescence intensity (AU)
50
45
40
35
30
25
20
15
10
5
0
*** *** *** ***
Vector
dyci-1(RNAi)
rab-7(RNAi)
dnc-1(RNAi)
rilp-1(RNAi)
C
wt
39aKO
BA:
- + - +
α-P-Beclin1
α-Beclin1
D
mCherry
mCherry::
DYNC1I2
Control
DYNC1I2
shRNA-4
E
mCherry::DYNC1I2
shRNA
- 1 2 3 4 5
Blot
α-mCherry
α-tubulin
mCherry
shRNA
- 1 2 3 4 5
α-mCherry
α-tubulin

Supplemental Figure 3. Deficiency in dynein *dyci-1/DYNC1I2* induces lysosome abnormalities. *A*) Disruption of *dyci-1* or *rab-7* by RNAi induces increase in the lysosome reporter *lmp-1::gfp* expression, while RNAi disruption of *dnc-1* (encoding dynactin) or *rilp-1* (encoding RAB-7 interacting protein) has no detectable effects on lysosome reporter levels, indicating subunit specificity of dynein/dynactin complex in regulating lysosome dynamics. Scale bar, 100 μm. *B*) Quantification of fluorescence intensity of lysosome reporter expression in wild-type and RNAi-treated animals. Data represents mean ± S.E.M.; ***, $P<0.001$. *C*) Western blot analysis showing enhanced phosphorylation of Beclin-1 on Ser15 in non-starved *TMEM39A* KO mutant cells, indicating inhibition of mTOR pathway in the absence of TMEM39A. *D*) Fluorescence compound images showing efficient knockdown of mCherry::DYNC1I2 but not mCherry expression in HEK293T cells expressing DYNC1I2-targeting shRNA. *E*) Western blot analysis showing efficient knockdown of mCherry::DYNC1I2 but not mCherry expression in HEK293T cells expressing DYNC1I2-targeting shRNA.

Movie Legends

Movie 1. Movie clip showing lysosome movement in the hypoderm of wild type animals that express ubiquitous lysosome reporter *rpl-28$_p$::lmp-1::Venus.* Each spherical dot represents a lysosome. Confocal images (Leica SPE, 40×) were taken every 15 seconds for 10 minutes and were compiled in FIJI (NIH) at 8 frames per second (fps) to generate the 5 second movie.

Movie 2. Movie clip showing tubular lysosomes in the hypoderm of *tmem-39* mutant animals that lack noticeable movement during the filming. Lysosome appears to accumulate in membranous structures as revealed by the ubiquitous lysosome reporter *rpl-28$_p$::lmp-1::Venus*. Confocal images (Leica SPE, 40×) were taken every 15 seconds for 10 minutes and were compiled in FIJI (NIH) at 8 frames per second (fps) to generate the 5 second movie.

Table S1. TMEM39A interacting proteins identified by yeast two-hybrid screens

Gene	Protein
ATP6V1B2	ATP6V1B2 protein, partial
CLTC	clathrin heavy chain 1 isoform X1
CRYAB	alpha-crystallin B chain isoform 1
CTSB	lysosomal proteinase cathepsin B
DYNC1I2	dynein, cytoplasmic 1, intermediate chain 2, isoform CRA_b
EXD2	alternative protein EXD2
IVNS1ABP	influenza virus NS1A-binding protein isoform X1
LIPA	lysosomal acid lipase/cholesteryl ester hydrolase isoform 2
LOC107987423	liver carboxylesterase 1-like
LYST	lysosomal-trafficking regulator isoform X4
MDC1	Chain A, Crystal Structure Of Mdc1 Tandem Brct Domains
MLH1	DNA mismatch repair protein Mlh1 isoform 6
MT1G	metallothionein 1E (functional), isoform CRA_b
MYCBP2	PREDICTED: E3 ubiquitin-protein ligase MYCBP2 isoform X23
NARS	asparagine--tRNA ligase, cytoplasmic
PCNX4	pecanex-like protein 4 isoform 2
PLA1A	phospholipase A1 member A isoform 3
SEC23A	protein transport protein Sec23A isoform X1
TTN	cytoplasmic FMR1-interacting protein 2 isoform c
TUSC3	tumor suppressor candidate 3 isoform X2

Supplemental References

1. S. Brenner, The genetics of *Caenorhabditis elegans*. *Genetics* **77**, 71-94 (1974).

2. C. Mello, J. Kramer, D. Stinchcomb, V. Ambros, Efficient gene transfer in *C.elegans*: extrachromosomal maintenance and integration of transforming sequences. *EMBO J.* **10**, 3959–3970 (1991).

3. R. S. Kamath, *et al.*, Systematic functional analysis of the *Caenorhabditis elegans* genome using RNAi. *Nature* **421**, 231–7 (2003).

4. J. Rual, *et al.*, Toward improving *Caenorhabditis elegans* phenome mapping with an ORFeome-based RNAi library. *Genome Res* **14**, 2162–8 (2004).

5. L. Cong, *et al.*, Multiplex genome engineering using CRISPR/Cas systems. *Science* (2013) https:/doi.org/10.1126/science.1231143.

6. S. Bolte, F. P. Cordelières, A guided tour into subcellular colocalization analysis in light microscopy. *J. Microsc.* (2006) https:/doi.org/10.1111/j.1365-2818.2006.01706.x.